https://doi.org/10.5194/cp-2024-42
Preprint. Discussion started: 20 June 2024

Climate of the Past
Discussions
Open Access

Orbital-scale climate dynamics impacts on Gzhelian peatland wildfire activity in the Ordos Basin

Wenxu Du[1], Dawei Lv[1*], Zhihui Zhang[1*], Munira Raji[2], Cuiyu Song[1], Luojing Wang[1], Zekuan Li[1], Kai Cao[1], Ruoxiang Yuan[1], Yuzhuang Sun[3]

[1] Shandong Provincial Key Laboratory of Depositional Mineralization and Sedimentary Minerals, College of Earth Sciences and Engineering, Shandong University of Science and Technology, Qingdao 266590, China

[2] Sustainable Earth Institute, University of Plymouth, Devon, United Kingdom

[3] College of Earth Science and Engineering, Hebei University of Engineering, Handan 056038, Heibei, China

*Corresponding author: College of Earth Sciences and Engineering, Shandong University of Science and Technology, Qingdao 266590, China.

E-mail addresses: lvdawei95@163.com (D. Lv), zhzhihui@sdust.edu.cn (Z. Zhang).

Abstract

The Carboniferous, an important coal-forming period in geological history, was characterized by extensive vegetation and high oxygen levels. Numerous wildfire evidence suggests that high frequency of wildfire occurred at that time, specifically in peatlands. However, the control mechanisms for changes in wildfire activity in peatlands during this period are still not clearly understood. In this study, evidence from the Gzhelian in the Ordos Basin, such as the inertinite/vitrinite (I/V) ratio, indicated the existence of different frequencies of wildfire activity at that time. The CaO/MgO and CaO/MgO • Al_2O_3 climate indicators revealed that high-frequency wildfires mainly occur in warm and humid climates. Based on former age constraints, we deduced that orbital cycles (long eccentricity) controlled the climate influence on peatland wildfires during

https://doi.org/10.5194/cp-2024-42
Preprint. Discussion started: 20 June 2024

the Gzhelian. When eccentricity was high, abundant sunshine and frequent rainfall led to warmer and more humid peatlands. The latter environments were more favourable for vegetation development, leading to increased fuel loads, which in turn led to more frequent wildfires. Moreover, the Gzhelian global wildfire records, showed that evidence of wildfire during this period was mainly located in areas with abundant tropical vegetation, supporting the view that wildfire activity during this period was mainly controlled by the fuel loads. Although Hg could be produced by peatland wildfires, but our results show that Hg was mainly from frequent volcanic activity during this period.

Keywords: Wildfire; Inertinite; Gzhelian; Hg; Long eccentricity

1. Introduction

In recent years, information about wildfires preserved in coal seams has been ~~exposed~~ (Robson et al., 2015; Hou et al., 2022; Zhang et al., 2022). ~~The macerals in the~~ pyrogenic inertinite (fossil charcoal in coal), such as fusinite, semifusinite, and inertodetrinite, have been widely used as direct evidence to demonstrate the occurrence of paleo-wildfires (Scott, 2010, 2022; Jasper et al., 2013; Belcher and Hudspith, 2017; Uhl et al., 2022; Shen et al., 2023). The Carboniferous through Permian were important coal-forming periods in geologic history where large deposits of coal developed (Berner, 2003). Although wildfires of the period have been somewhat summarized by previous authors (e.g., Scott, 2000; Glasspool and Scott, 2010; Glasspool et al. 2015; Jasper et al. 2021), there is a dearth of high-resolution wildfire records from the period. Glasspool et al. (2015) concluded from the analysis of the inertinite in coal that the frequency of wildfires during the Late Paleozoic was mainly due to the higher oxygen content in the atmosphere at that time. However, more detailed controlled factors for Carboniferous through Permian wildfires need to be improved.

Many researchers have found that changes in charcoal abundance in sediments indicate

https://doi.org/10.5194/cp-2024-42
Preprint. Discussion started: 20 June 2024

changes in orbital cycle forcing climate change, which in turn influences wildfire activity (Verardo and Ruddiman, 1996; Thevenon et al., 2004; Hao et al., 2020; Shi et al., 2020; Cheng et al., 2022). Daniau et al. (2013) found that the past 170 kyr of grassland wildfire activity in southern Africa has been controlled by precession. Zhang et al. (2020a, 2023) found that wildfire activity during the Early to Middle Jurassic was influenced by changes in long eccentricity (405 kyr) and the precession cycle. ~~The orbital period~~ (eccentricity, obliquity, and precession) force~~s~~ climate change, thus affecting the amount and flammability of vegetation fuels to control wildfire activity (Zhou et al., 2023). ~~The study of whether~~ wildfire activity in Carboniferous to Permian peatlands was controlled by changes in orbital cycles is unclear. Late Carboniferous Gzhelian global wildfire records indicate that ~~the~~ wildfire ~~records~~ were all distributed in tropical climate zones. Tropical climate zones ~~have~~ abundant fuel accumulation and orbital cycle forcing wildfire activity ~~may be more pronounced~~ (DiMichele, 2014).

As the largest Late Carboniferous to Early Permian peat basin in China, the Ordos Basin contain~~ed~~ a large amount of coal ~~seams~~, ~~which were~~ preserved with numerous volcanic ~~ashes~~ and wildfire products in the coal seams (Wang, 2017; Xu et al., 2020; Zhao et al., 2023; Zhang et al., 2023a, 2023b). In this paper, the focus is on the No. 9 coal of the Yaogou Coal Mine in the Jungar Coalfield of the Ordos ~~torder~~ to understand the occurrence of the Late Carboniferous wildfires and the variation of burning temperatures. Employing the clear age constraints of the No.9 coal seam, the possible role of long eccentricity orbital cycle changes in driving wildfires by means of wildfire frequency and climate indicators at that time can be explored (Zhang et al., 2023a). Volcanic activity, frequent wildfires, and other causes can lead to Hg enrichment, and this study also explores the relationship between wildfire activity, volcanic activity, and Hg at that time, using changes in Hg content in No. 9 coal.

https://doi.org/10.5194/cp-2024-42
Preprint. Discussion started: 20 June 2024

Climate of the Past
Discussions
Open Access

2. Geological setting

The Ordos Basin, located at the western margin of the North China Craton, is the second largest terrestrial sedimentary basin in China (Ao et al., 2012; Zhang et al., 2023a). The Jungar Coalfield is in the southwestern part of the Inner Mongolia Autonomous Region of China ~~and~~ in the northeastern part of the Ordos Basin, ~~which~~ contains about 26.8 Gt of coal reserves, which is one of the richest coal reserves in northern China (Dai et al., 2006,2008,2012; Li et al., 2016). The coalfield contains coal-bearing sequences of the Carboniferous and Permian systems (Wang et al., 2011).

This study was conducted in the Yaogou Mine, in the northeastern part of the Jungar Coal Field (Fig. 1b). The coal-bearing sequences in the Yaogou Mine include the Benxi Formation, Taiyuan Formation, and Shanxi Formation, with a total thickness of 84~200 m (Zhang et al., 2023a). The Benxi Formation, with a total thickness of 84~200 m (Zhang et al., 2023a), lies unconformably on the Middle Ordovician Majiagou Formation, with a thickness of about 17~28 m. The Taiyuan Formation is underlying by the Benxi Formation. The Taiyuan Formation, with a thickness of about 31-75 m (average 58 m), conformably overlies the Benxi Formation. The Taiyuan Formation consists mainly of grey and gray-white quartz sandstone, siltstone, mudstone, and five coal beds marked from top to base as No. 6 to No. 10 (Fig. 1c) (Zhang et al., 2023a). Zhang et al. (2023a) determined by U-Pb zircon from altered volcanic ashes at the top and bottom of No. 9 coal that the Taiyuan Formation in this study area belongs to the Gzhelian stage of the Late Pennsylvanian. The Shanxi Formation with a thickness of about 35-97 m is mainly terrigenous coal-bearing clastic rocks, dominated by sandstones and coal seams (Zhang et al., 2023a).

https://doi.org/10.5194/cp-2024-42
Preprint. Discussion started: 20 June 2024

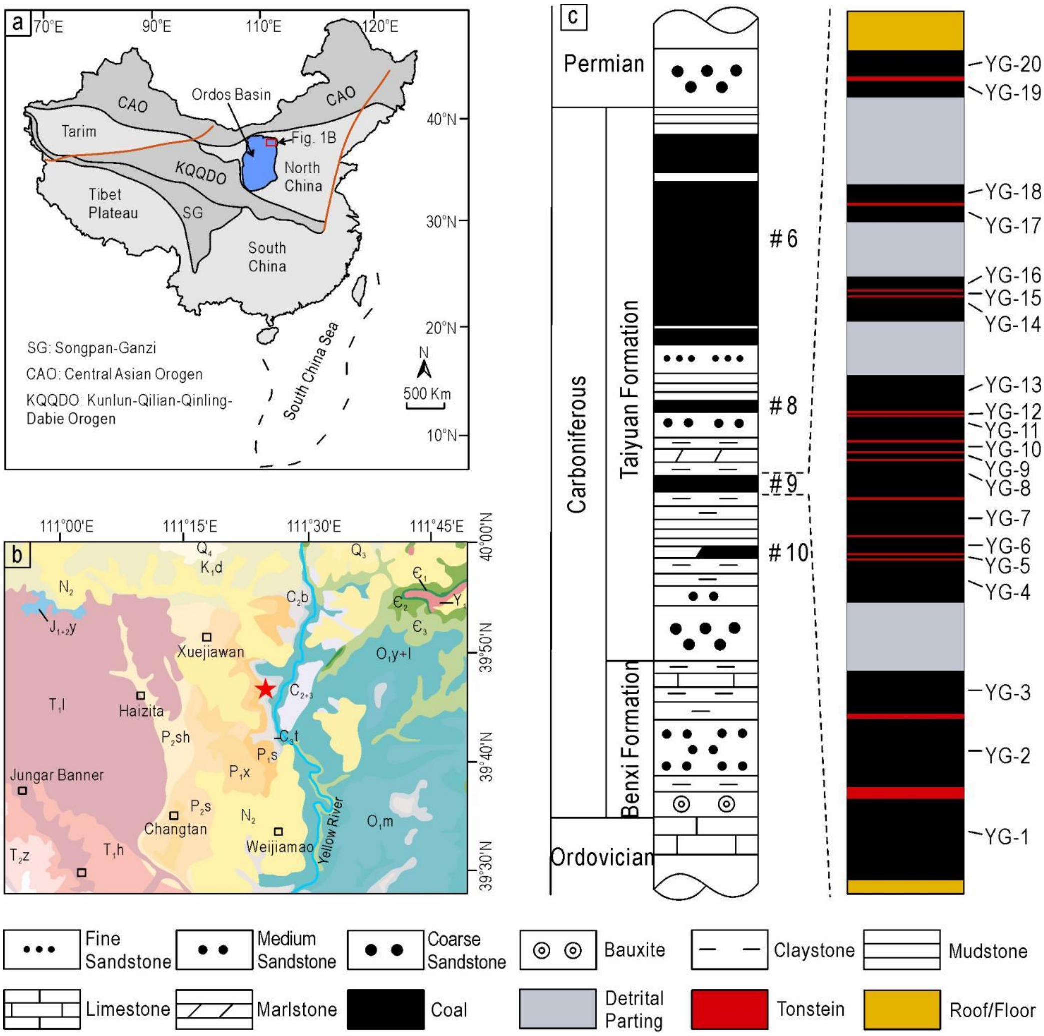

Fig. 1 Comprehensive geologic map of the Yaogou coal mine in the Ordos Basin, northern China. (a) Map showing the location of the Ordos Basin and the study area. (b) Geologic map of the study area showing the location of the study area (red stars). (c) Sedimentary sequence of the Jungar Coal Field and columnar map of the No. 9 coal seam. The No. 9 coal occurs in the Taiyuan Formation. Q_4-Holocene, Q_3-Pleistocene, N_2-Pliocene, K_1d-Dongsheng Formation (Fm.), J_{1+2}y-Yan'an Fm., T_2z-Zhifang Fm., T_1h-Heshanggou Fm., T_1l-Liujiagou Fm., P_2sh-Shiqianfeng Fm., P_2s-upper Shihezi Fm., P_1x-lower Shihezi Fm., P_1s-Shanxi Fm., C_3t-Taiyuan Fm., C_2b-Benxi Fm., O_1m-Majiagou Fm., O_1y+l-Yeli and Liangjiashan Formations. Figure modified from Zhang et al. (2023a).

https://doi.org/10.5194/cp-2024-42
Preprint. Discussion started: 20 June 2024

3. Material and methods

3.1 Sampling

In this study, a total of 20 coal samples were collected from the exposed face of the No. 9 coal at the Yaogou Mine, with a cumulative thickness of the profile of about 6.1 m. To minimize contamination and oxidation, the samples were all immediately stored in plastic bags. From bottom to top, all coal samples were marked YG-1 to YG-20 (Fig. 1c).

3.2 Analytical method

The analytical methods used in this study to demonstrate wildfire characteristics included petrographic analysis, coal rock micro component identification, fusinite reflectance measurements, and scanning electron microscopy (SEM).

The collected fossil charcoal fragments were crushed to a < 20 top size and the crushed samples were embedded in epoxy resins. The reflectance of the fusinite was measured ~~by the~~ oil immersion at room temperature and determined using an MSP UV-VIS2000 spectrophotometer (Petersen and Lindström, 2012; Xu et al., 2020). To estimate the wildfire burning temperatures represented by the experimental samples, calculations were based on the correlation proposed by previous works:

$$T=184.1+117.76\times\%R_o, \qquad (1)$$

with R_o represents the reflectance of the inertinite (Jones, 1997; Petersen and Lindström, 2012). Based on the model of oxygen content proposed by Glasspool (2010, 2015), the oxygen content in the atmosphere was predicted for the period of this study:

$$I=(0.5-0.5\cos[\pi(O-O_{min})/(O_{max}-O_{min})])^n, \qquad (2)$$

with I as the average inertinite content, O as the oxygen content, O_{max} as the oxygen content when the inertinite content reached 100%, and O_{min} as the oxygen content when was no inertinite.

https://doi.org/10.5194/cp-2024-42
Preprint. Discussion started: 20 June 2024

The microstructure of fossilized charcoal samples was observed by SEM to ~~make a clearer observation~~ of fossilized charcoal samples. The samples were observed under vacuum conditions using a 10 kV accelerating voltage, standard beam light, and a secondary electron probe. All the above experiments were completed at the Shandong Provincial Key Laboratory of Depositional Mineralisation and Sedimentary Minerals, Shandong University of Science and Technology.

To determine ~~the coal rock components,~~ the coal samples taken were measured according to the National Standard GB/T8899-2013. ~~The reflectivity of the vitrinite group of the coal samples~~ was measured according to the National Standard GB/T 6948-2008. To improve the quantification of charcoal abundance in each single sample, the ratio between inertinite maceral and vitrinite macerals (I/V), was calculated to determine the frequency of wildfires (Zhang et al., 2022). All of the latter experiments were completed ~~in~~ Xi'an Coal Science and Technology Ltd. All samples were analyzed for Total Organic Carbon (TOC) according to the National Standard GB/T19145-2003. ~~All samples were analyzed for~~ Hg concentration according to the National Standard GB/T 22105.1-2008. All above experiments were completed at the Beijing Qingchen Huanyu Petroleum Geological Technology Co. Ltd.

3.3 Data Synthesis

To build a reliable database of the Gzhelian wildfire evidence, data was compiled from peer-reviewed journal publications following the program of Lu (2021) and Lv (2024). Personal data and unpublished materials were not included in our study. ~~We used the keywords 'Gzhelian wildfire', 'charcoal', 'inertinite', 'fusain', 'fusinite', and/or 'PAHs' to search papers in Google Scholar, Web of Science, ScienceDirect, and JSTOR.~~ Literature searches were conducted ~~by the end of April 2024~~.

To minimize the possibility of ~~low credible/reliable~~ wildfire data, the data published in the

https://doi.org/10.5194/cp-2024-42
Preprint. Discussion started: 20 June 2024

original article was double-checked and evaluated before inclusion in our database. The evidence for fossil charcoal in the database is based on the standardized guidelines in Scott (2000,2010,2020). The distinction between sources of PAHs (pyrogenic and petrogenic) was made according to Yunker et al. (2002), and only records of pyrogenic PAHs were included. For example, Hower et al. (2022) had ~~two~~ inertinite data that did not have details of where samples were taken, so they were discarded. The inertinite in Presswood et al. (2016) was due to magmatic intrusion, so it was discarded.

Three types of Gzhelian wildfire evidence were included in the database: charcoal type I (pyrogenic inertinite macerals from coals), charcoal type II (fossil charcoal from clastic sediments), and pyrogenic PAHs. The location (e.g., country, state/province, city, latitude, longitude, etc.), palaeogeographical localities (e.g., palaeocontinents, palaeolatitude, and palaeolongitude), stratigraphic unit (e.g., formation, group), and rock type (e.g., coal, sandstone, mudstone) were integrated for each wildfire record. When multiple studies reported wildfire data from the same geologic unit in the same location (e.g., section, region, or basin), they were considered as one record (Lu et al., 2021). Depending on the type of evidence, wildfire occurrences in the same study site can be identified in different studies and recorded as one occurrence.

The GPlates 2.2.0 model constructed by Scotece (2008) was used to estimate paleolatitudes and paleolongitudes data for wildfire occurrence. To provide a visual representation of the spatial distribution, the occurrence of wildfires was projected on a paleogeographic map of Gzhelian by Scotese (2021) (Fig. 9).

4. Results

4.1 Coal rock micro component and geochemical characterization

~~The microscopic component contents of the coal samples collected in the mineral-free state~~

https://doi.org/10.5194/cp-2024-42
Preprint. Discussion started: 20 June 2024

Climate of the Past
Discussions
Open Access
EGU

from No.9 coal of Yaogou Mine are shown in Table 1. ~~Of all the samples, the vitrinite~~ was dominant, with contents ranging from 64.5% to 84.7% (average = 73.5%). The inertinite content of the coal samples ranged from 14.1% to 30.8%, with an average content of 22.3%. ~~The liptinite had the lowest content~~, ranging from 1.3% to 8.7%, with an average content of 4.2%. Nearly all inertinite preserved in coal was defined as an incomplete combustion product, comparable to fossil charcoal (Scott 2000, 2010; Scott and Glasspool 2006, 2007; Diessel, 2010). Because of this, subcomponent analyses were analyzed ~~for the inertinite in the coal samples Table 1~~. ~~In the 20 coal samples, the~~ main component of the inertinite was semifusinite, with contents ranging from 7.4% to 17.2% ~~with~~ an average content of 11.5%. The content of inertodedetrinite was rather low, ranging from 1.8% to 13.4%, with an average content of 6.6%. The contents of fusinite, macrinite, and micrinite were low, with average contents of 1.2%, 2.3% and 0.7%. Among the 20 samples, the variation of inertinite/vitrinite ranged from 0.17 to 0.47, with a mean value of 0.31. The reflectance (R_{vo}) of the vitrinite of the 20 coal samples ranged from 0.37% to 0.66.

The TOC content of the 20 coal samples from the Taiyuan Formation ranged from 27.82% to 48.07%, with an average content of 39.49% (Table 2). The Hg content of the 20 samples varied greatly, ranging from 29.5 ppb to 393 ppb, with an average of 134.96 ppb (Table 2). Zhang et al. (2023a) analyzed the sulfur content, Al_2O_3 content, and ash yield of 20 coal seams in the Taiyuan Formation in this study area (Table 2). The Spearman correlation ~~analysis showed that the correlation~~ between Hg and Al_2O_3 in the 20 coal samples from Taiyuan Formation is ~~highly~~ significant, with positive correlation, the correlation coefficient is ~~+~~0.529, and ~~the~~ significance is 0.016 (Fig. 6a). The correlation between Hg and sulfur is not significant with ~~the~~ correlation coefficient of -0.175 and significance of 0.46 (Fig. 6b). The correlation between Hg and TOC is significant, with a correlation coefficient of -0.659, and ~~the~~ significance is 0.002 (Fig. 6c). Since the

https://doi.org/10.5194/cp-2024-42
Preprint. Discussion started: 20 June 2024

source of elemental aluminum in coal is mainly clay minerals, the correlation between elemental Al and ash yield was analyzed. The correlation between elemental Al and ash yield in the coal samples of this study was highly significant with a correlation coefficient of +0.776 and significance of 0. The correlation between elemental Hg and ash yield was significant and positive with the correlation coefficient of +0.481 and significance of 0.032 (Fig. 6d).

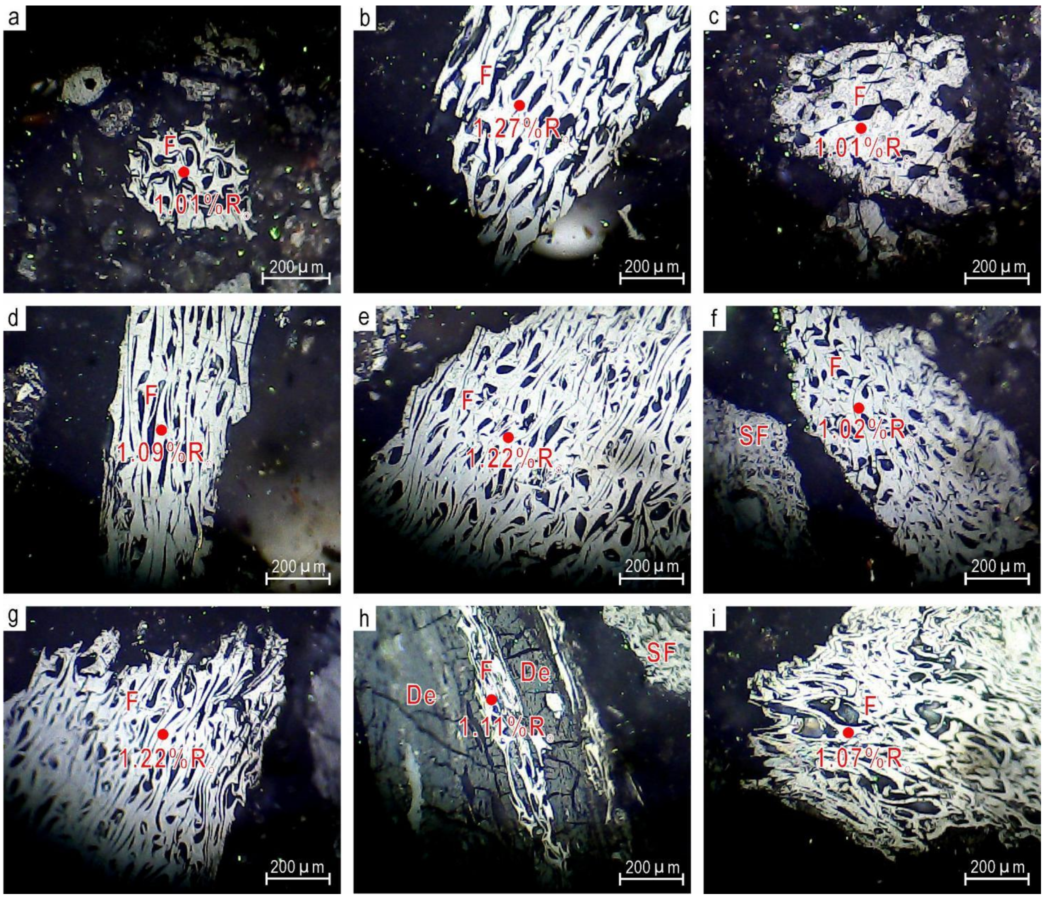

Fig. 2 Features of fossil charcoal in the Ordos Basin Taiyuan Formation observed under the oil immersion optical microscopy. F-fusinite; SF-semifusinite; Red circles show the test points, and numbers show the reflectance values of the points.

https://doi.org/10.5194/cp-2024-42
Preprint. Discussion started: 20 June 2024

Climate of the Past Discussions

Table 1

The coal micro component contents of 20 seams of No. 9 coal from Yaogou Mine in Ordos Basin

Sample No.	Percentage of the total organic macerals (vol.%)			Percentage of the total inertinite macerals (vol.%)					TOM (vol.%)	Total minerals (vol.%)
	Vitrinite	Inertinite	Liptinite	Fusinite	Semifusinite	Macrinite	Micrinite	Inertodetrinite		
YG-1	79.6	14.6	5.8	1.1	9.3	0	0.2	4	53.9	46.1
YG-2	80.5	16	3.5	2.4	10.6	0.6	0.6	1.8	60.4	39.6
YG-3	68.3	27.4	4.3	0.9	14.1	1.5	2.6	8.3	81.2	18.8
YG-4	64.5	26.8	8.7	0.4	13.3	2.4	0.4	10.3	84.8	15.2
YG-5	84.7	11.9	3.4	0.4	7.4	1.5	0.2	2.4	84.9	15.1
YG-6	65.2	30.8	4	0	14.6	2.4	0.4	13.4	86.2	13.8
YG-7	72.2	23	4.8	3	10.7	3	0.8	5.5	87.1	12.9
YG-8	70.8	21.5	7.7	2.5	12.2	1.5	0.2	5.1	81.8	18.2
YG-9	78.4	19.1	2.5	0	9.8	2.5	0.4	6.4	80.1	19.9
YG-10	66.1	27.4	6.5	3.8	13.1	3.2	0.6	6.7	83.9	16.1
YG-11	75.2	23.5	1.3	0.6	12	3.4	0.2	7.3	79.6	20.4
YG-12	72.1	25.1	2.8	0.9	15.4	2.2	0.4	6.2	73.9	26.1
YG-13	65.8	30.2	4	0.8	17.2	4.1	1.8	6.3	86.2	13.8
YG-14	82	14.1	3.9	0	8.3	2.1	0	3.7	81.3	18.7
YG-15	80.2	18.4	1.4	0	11.2	0.8	0.6	5.8	77	23
YG-16	81.8	16.5	1.7	0	10.4	1.2	1.2	3.7	85.2	14.8
YG-17	78.1	18.4	3.5	2.7	9	1.7	0.5	4.5	59.5	40.5
YG-18	66.8	28.9	4.3	0.8	11.3	4.7	0	12.1	59.9	40.1
YG-19	73	24.9	2.1	1.1	8.9	2.9	0.4	11.6	71.5	28.5
YG-20	65	27.2	7.8	3.2	11	4.1	2	6.9	81.8	18.2

https://doi.org/10.5194/cp-2024-42
Preprint. Discussion started: 20 June 2024

Table 2

The chemical element data of 20 coal seams from the No. 9 coal of the Yaogou coal mine in the Ordos Basin. The Al_2O_3, TS, and TOC were from Zhang et al. (2023a).

Sample	Hg (ppb)	Al_2O_3 (%)	TS (%)	TOC (%)
YG-1	255	16.33	0.23	27.82
YG-2	145	11.94	0.39	29.92
YG-3	63.2	7.67	0.44	47.30
YG-4	118	9.46	0.77	44.14
YG-5	58.6	8.96	0.32	48.07
YG-6	70.4	12.75	0.41	42.04
YG-7	85.1	7.44	0.57	44.72
YG-8	35.4	7.42	0.52	48.04
YG-9	43.5	11.87	0.45	41.17
YG-10	269	10.5	0.59	41.51
YG-11	88.5	10.53	0.48	38.10
YG-12	83.9	10.74	0.5	35.33
YG-13	34.5	9.57	0.48	46.26
YG-14	156	12.77	0.35	40.37
YG-15	352	16.48	0.42	32.35
YG-16	237	14.23	0.32	36.72
YG-17	393	12.42	0.36	29.26
YG-18	152	17.88	0.29	32.05
YG-19	29.5	13.53	0.3	37.95
YG-20	29.6	7.57	0.44	46.68

4.2 Microscopic observations of fossil charcoal

Under the oil-immersion reflected-light microscope, a large amount of semifusinite was observed in the coal samples of the Taiyuan Formation. Some representative ~~micrographs~~ are provided in Fig. 2. The pore sizes of the semifusinite ranged from 40 - 120 μm , with a small variation in pore size. The measured reflectance of the inertinite of 20 coal samples from the Taiyuan Formation ranged from 1.01% to 2.07%, with the average value of 1.66%.

The structural features of the fibre structure and the cell wall in the fossil charcoal fragments can be observed by SEM. The majority~~t~~ of the cellular structures were crushed or broken(Fig. 3a,c). As shown by the radial structure, the tubular cells were straight and 10-20 μm wide (Fig. 3a). There was one single row of circular or elliptical pitting with 0.5-2 μm width (Fig. 3b). ~~And~~ the cell walls

https://doi.org/10.5194/cp-2024-42
Preprint. Discussion started: 20 June 2024

Climate of the Past Discussions
Open Access
EGU

of the samples showed homogenization (Fig. 3d).

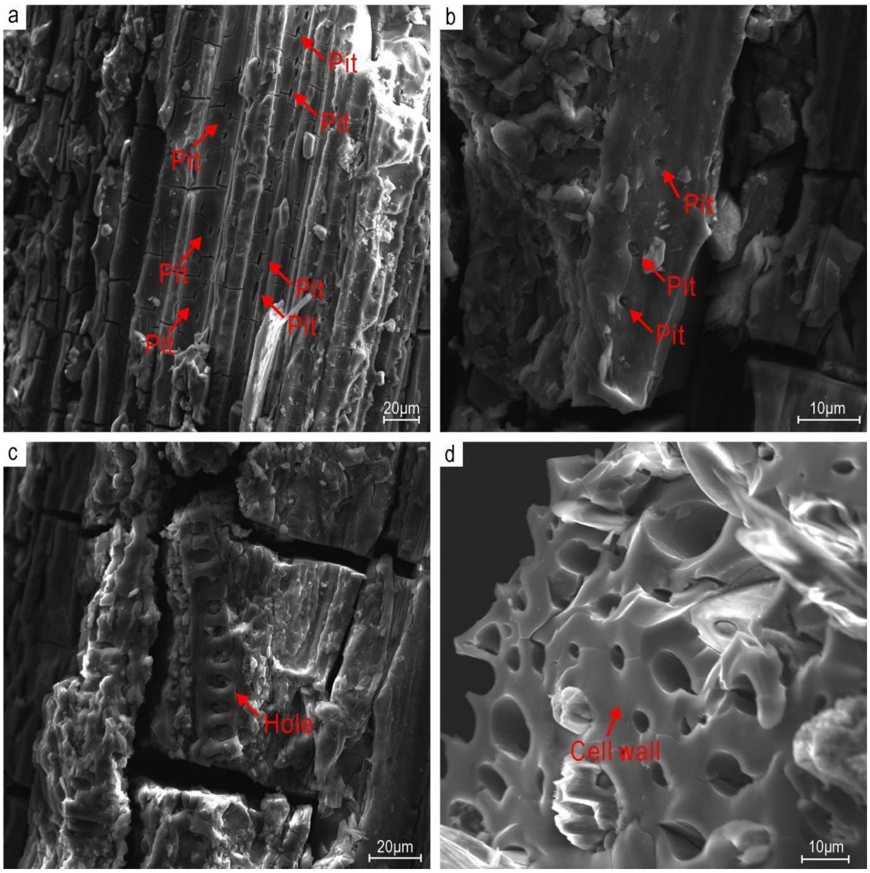

Fig. 3 Scanning electron microscope electron probe image of fossilized charcoal. (a-b) Red arrows point to uniseriate pits. (c) Red arrow points to larger ~~holes~~ in the cell wall that may represent pits, which were diagenetically enlarged during charring. (d) Red arrow points to homogenized cell wall.

4.3 The Gzhelian wildfire record in geologic context

Published wildfire records for the Gzhelian were compiled in Table S1. Based on the type of evidence these can be divided into five groups: 23 records of charcoal type I (79.4% of the total records), two records of charcoal type II (6.9%), one record of pyrogenic PAHs (3.4%), two records of charcoal type I and charcoal type II (6.9%), and one record of charcoal type II and pyrogenic PAHs (3.4%). The published Gzhelian wildfire data ~~were observed in~~ 19 geologic units (or

https://doi.org/10.5194/cp-2024-42
Preprint. Discussion started: 20 June 2024

formations), with two record from an unclear unit.

All of the 29 reported Gzhelian wildfires have occurred in ~~the~~ lower latitudes (30°N-30°S) (Fig. 9). According to Boucot et al.'s (2013) suggested paleoclimatic classification, the Gzhelian can be divided into four different paleoclimatic zones: cool temperate, warm temperate, arid and tropical. The Gzhelian wildfires all occurred in the tropical area (Fig. 9).

5. Discussion

5.1 Repeated wildfire in the Gzhelian of the Ordos Basin

The origin of the inertinite in coal has been controversial, and it has been suggested that the fusinite and semifusinite in the inertinite may be produced from fungal degradation of vegetation tissues in oxidizing environments or influenced by other microbial activities (Beeston, 1987; Teichmüller, 1989; Varma, 1996; ICCP, 2001). Some semifusinite in coal may also have been formed during diagenesis (Hudspith and Belcher, 2020). Nevertheless, research suggests that the fusinite and semifusinite in coal ~~were equivalent to~~ fossil charcoal (Scott and Glasspool, 2007; Hudspith et al., 2012), which was produced by the incomplete combustion of vegetation by wildfires (Scott, 2010; Liu et al., 2022). All coal samples from the Taiyuan Formation had low levels of both macrinite and micrinite (Table 1). Both fusinite and semifusinite preserved ~~complete~~ cellular structures (Fig. 2), suggesting that the fusinite and semifusinite in the study samples ~~may be~~ products of vegetation combustion.

In addition, the low reflectance of the vitrinite in the coal samples, averaging 0.49%, indicated that the samples were ~~poorly metamorphosed,~~ and was not enough to support the claim that the semifusinite in the samples was due to diagenesis. Experiments ~~had~~ shown that the carbonization temperature for homogenization of vegetation cell walls needs to be ~~at least~~ higher than 250 - 300 °C (Scott and Jones, 1991; Osterkamp et al., 2017). Obvious homogenization of the cell walls of the

https://doi.org/10.5194/cp-2024-42
Preprint. Discussion started: 20 June 2024

fossil charcoal could be observed under the SEM (Fig. 3d), which more clearly suggested that the fossil charcoal in the samples was caused by wildfire burning. The inertinite content of the Taiyuan Formation coal samples showed a small range of variability (14.1% - 30.8%) and was dominated by semifusinite (7.4% - 17.2%), which indicates the presence of frequent small wildfires during this period. Under the SEM, it can be observed that the cellular structure of the fossil charcoal from the Taiyuan Formation is obviously broken, and some cellular cavities in the charcoal appeared to have different degrees of deformation (Fig. 3c), which may be due to the tectonic movement of the strata.

Scott (2010) divided wildfires into three types based on their strength: surface fire, ground fire, and crown fire. Among these, surface fires whose fuels are mainly surface herbaceous, shrubs and various biological wastes, burn at lower temperatures, usually below 400 ^{o}C. Ground fires whose fuel is mainly the dry humus layer in the soil, which can burn thick layers of peat, burn at relatively high temperatures, up to 600 ^{o}C. It has been demonstrated that the reflectance of the inertinite is positively correlated with the combustion temperature, with higher inertinite reflectance indicating higher combustion temperatures (Jones et al., 1991; Guo and Bustin, 1998; Scott and Glasspool, 2007; McParland et al., 2009). The reflectance of the inertinite in the Taiyuan Formation samples varied in a small range (1.01%-2.07%), and it can be inferred that the Taiyuan Formation wildfire burned at temperatures ranging was about 300 ^{o}C to 430 ^{o}C, with an average burn temperature of 379 ^{o}C (after formula Scott and Glasspool, 2015). This suggests that mainly low-temperature fires occurred in the Ordos Basin during the Gzhelian (Fig. 4). Wildfire burning may have been fueled primarily by low-growing vegetation or biological waste, which would be consistent with the homogenization of fern cell walls observed under the SEM.

https://doi.org/10.5194/cp-2024-42
Preprint. Discussion started: 20 June 2024

Climate of the Past
Discussions
Open Access

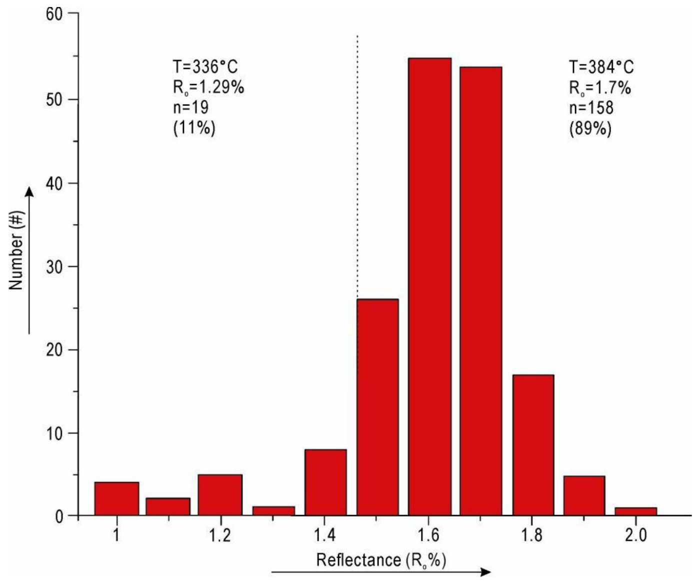

Fig. 4 The inertinite reflectance histograms indicate calculated combustion temperatures (Shukla et al., 2023).

5.2 Sources of elemental mercury in coal

Soils are the largest global reservoir of Hg and forest ecosystems are one of the key areas in the Hg cycle (Wang et al., 2019). Peatland vegetation can retain atmospheric Hg in their bodies by absorbing it (Grigal, 2003), while humus and sulfides in peatlands have a high affinity for Hg, which makes them important sinks for Hg (Yudovich and Ketris, 2005; Woerndle et al., 2018). In the pre-anthropic era, the main sources of Hg in the surface environment were volcanic eruptions, intense continental weathering, and wildfires (Pavlish et al., 2003; Pyle and Mather, 2003; Selin, 2009; Shen et al., 2020).

In this study, Hg was negatively correlated with Total Organic Carbon (TOC) and Total Sulfur (TS) (Fig. 6), indicating that Hg is not predominantly present in organic matter and sulfides. Correlation of elemental concentration with ash yield may provide preliminary information on their affinity with organic and inorganic (Eskanazy et al., 2010; Kortenski and Sotirov, 2002; Dai et al., 2012a; Zhang et al., 2023a). Mercury has a relatively high correlation (r=0.481) with ash yield, indicating a dominant inorganic affinity. There was a high correlation between Hg and Al_2O_3 in this study (r=0.529), indicating that Hg was mainly enriched in clay minerals (Fig. 6). The Hg concentrations in coal samples YG-1, YG-10, YG-15, YG-16, and YG-17 (237-352 ppb) were generally higher than the average concentration of coals from around the world (100 ppb) and the average concentration of Chinese coals (163 ppb) (Dai et al., 2012b). After normalizing for Al_2O_3, it still showed anomalously high values in these five coal samples, indicating that these five Hg peaks are true Hg anomalies (Fig. 5) (Xie et al., 2022).

Xie et al. (2022) demonstrated that wildfire burning resulted in the release of most of the Hg accumulated in vegetation and soils to the atmosphere, and that atmospheric Hg accumulated quickly in peatlands, leading to Hg anomalies enrichment in peatlands. Comparing the Hg levels of the samples in this study with the frequency of wildfires ~~has not shown that~~ the anomalously high values of Hg ~~are well correlated with the frequency of wildfires~~ (Fig. 5). There were even anomalously high values of Hg in samples YG-15, YG-16, and YG-17, but the frequency of wildfires was significantly reduced. This indicates that the anomalous enrichment of Hg in this study was not caused by wildfire burning.

The mass of Hg in forest vegetation is about 0.1 mg/m^2 , however, the mass of Hg in peatlands is about 20 mg/m^2 , which is much greater than the amount in vegetation (Grigal, 2003; Turetsky et al., 2006). The types of wildfire burning in Xie et al. (2022) were primarily ground and surface fires. Ground fires were fueled primarily by a dry humus layer in the soil (Scott, 2010), which can burn a thicker layer of peat, resulting in the release of Hg from the peatland. In this study, the type of wildfire burning was predominantly surface fires, with the primary fuels for surface fires were low surface vegetation and biological litter (Scott, 2010), which coincides with the observation of ferns as fuels in the SEM (Fig. 3). Ku et al. (2018) found that different wildfire intensities had different effects on Hg volatilization from vegetation. Therefore, wildfire burning may not necessarily lead to

https://doi.org/10.5194/cp-2024-42
Preprint. Discussion started: 20 June 2024

Hg enrichment, and wildfire types may not have the same effect on Hg. Mercury enrichment is favored when wildfires were primarily ground fires, where burning of the peat layer resulted in the release of large quantities of Hg, which were absorbed by the peatland.

Excluding the anomalous enrichment of Hg in coal due to wildfire activities, the known causes of the anomalous enrichment of Hg in coal are mainly the volcanic activities during the early peatland accretionary phase that led to the increase of Hg input (Roos-Barraclough et al., 2002; Yudovich and Ketris, 2005), and the invasion of low-temperature hydrothermal and magmatic fluids into coal-bearing strata (Sun et al., 2016; Zheng et al., 2018). Zhang et al. (2023a) identified 15 altered volcanic ashes in this study area, demonstrating the frequent volcanic activity during this depositional time. And it was confirmed that trace element enrichment in closed coal seams may be due to the dipping of tonsteins by acid solutions. Correlation analysis of the Hg content of No. 9 coal with trace elements such as Ga, Zr, and Hf revealed a significant correlation (r=0.581-0.705). Hg enrichment has been widely used as the indicator of volcanic sediment input (Shen et al., 2020), so the anomalously high values of Hg in the study area may be attributed to the input of Hg elements due to the frequent volcanic activities at that time, and the Hg in the tonsteins was leached into the closing coals by leaching of the acid solution.

https://doi.org/10.5194/cp-2024-42
Preprint. Discussion started: 20 June 2024

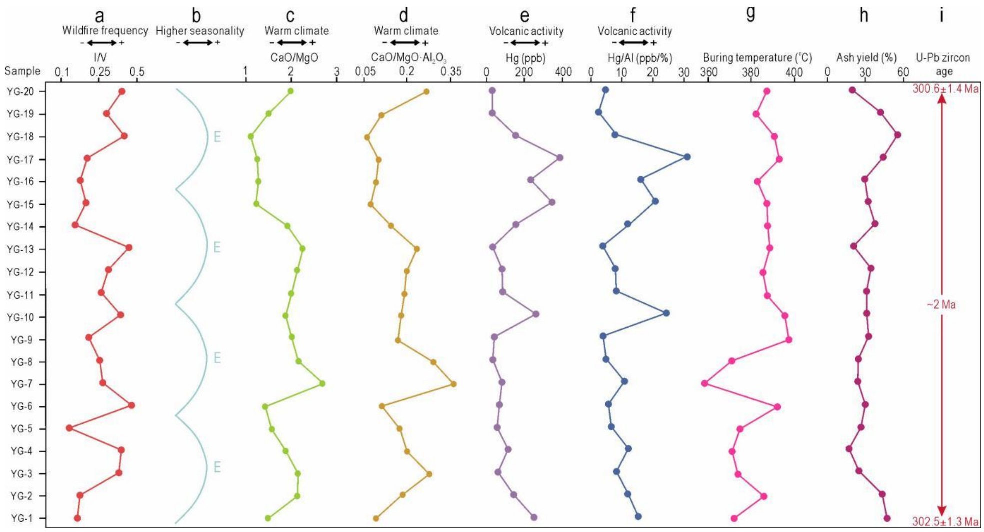

Fig. 5 Comprehensive analysis map of No.9 coal in Yaogou Mine. (a) Inertinite/ Vitrinite variations in 20 coal samples. (b) Long eccentricity orbital cycle variation. (c) CaO/MgO trends in 20 coal samples. (d) CaO/MgO • Al_2O_3 trends in 20 coal samples. (e) Hg content trends in 20 coal samples. (f) Hg/Al trends in 20 coal samples. (g) Combustion temperature trends in 20 coal samples. (h) Ash yield trends in 20 coal samples. (i) Age of No. 9 coal, referred to Zhang et al. (2023a).

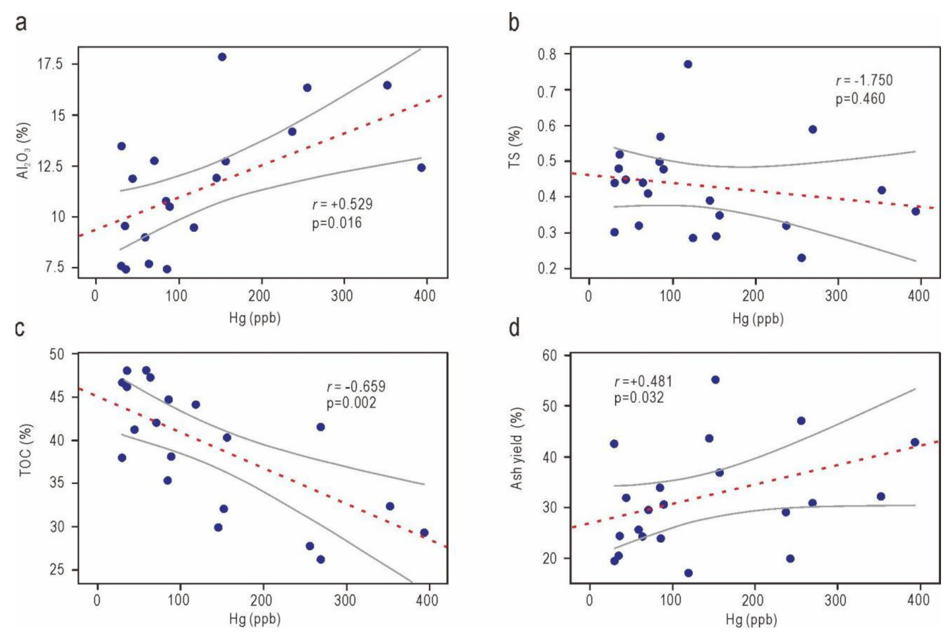

Fig. 6 (a) Correlation between Hg and Al_2O_3. (b) Correlation between Hg and TS. (c) Correlation between Hg and

https://doi.org/10.5194/cp-2024-42
Preprint. Discussion started: 20 June 2024

TOC. (d) Correlation between Hg and ash yield. Spearman's P and r values are shown. Red lines denote the best-fit linear regression line. Gray curve lines denote the 95% confidence interval.

5.3 Gzhelian wildfires and climate change

5.3.1 Regional wildfire trends

Wildfire activity during geologic history has been influenced primarily by changes in atmospheric oxygen levels, climate and vegetation (Belcher and Hudspith, 2017; Baker, 2022). For example, Glasspool and Scott (2010) suggested that high levels of oxygen in the atmosphere ~~influence~~ increased wildfire activity on different time scales. Baker (2022) found that past periods of global climate change on Earth have been accompanied by increased wildfire activity. Vegetation type changes also influence wildfire occurrence, for example, the rise of angiosperms during the Cretaceous may have led to an increase in wildfire activity at that time (Lü et al., 2024).

The level of oxygen in the atmosphere plays a key role in the occurrence of wildfires (Scott, 2000); when oxygen levels are below 15% it will not be possible to sustain vegetation burning, and when levels are above 23% humid vegetation will continue to burn. Based on model predictions, the oxygen level of 24.6% in the Gzhelian is higher than current oxygen levels and can sustain wildfire burning in humidter environments (Fig. 7).

CaO/MgO can be used as an indicator for paleoclimate reconstruction (Chen and Wan, 1999; Sun et al., 2010; Liu et al., 2013; Fu et al., 2018), and the ratio of CaO/MgO • Al_2O_3 ~~can more sensitively respond to the~~ temperature changes ~~at that time~~, with high values ~~indicated for~~ warm periods, and low values ~~indicated for~~ cold periods (Chen and Wan, 1999; Fu et al., 2018; Zhang et al., 2020b; Zhang et al., 2021). In this study, periods of high wildfire frequency (e.g., YG-10, YG-11, YG-12, YG-13) had higher values of CaO/MgO and CaO/MgO • Al_2O_3, ~~indicated~~ of a warm and humid climate (Fig. 5). Periods of lower wildfire frequency (e.g., YG-14, YG-15, YG-16, YG-17)

https://doi.org/10.5194/cp-2024-42
Preprint. Discussion started: 20 June 2024

had lower CaO/MgO and CaO/MgO • Al_2O_3 values, indicated a cold and dry climate (Fig. 5). Although wildfires were more easily caused when the climate was dry, cold climates with lower temperatures were not favourable for vegetation development (Brovkin, 2002), and a dryer climate meant less rainfall, both of which led to a decrease in fuels, hence a less frequent occurrence of wildfires. However, in warm and humid climatic periods, where seasonal variations were stronger, sufficient rainfall and suitable temperatures promote the development of vegetation, leading to a significant accumulation of fuels, hence more favourable for wildfires to occur (Litt et al., 2014; Stockhecke et al., 2016; Swain, 2021). Furthermore, previous research has found that high frequencies of wildfire activity have occurred in moderately humid environments (Daniau et al, 2012; Marlon et al, 2013). This study predicts oxygen levels sufficient to sustain wildfires in humid conditions for sustained burning, so sufficient fuel accumulation may have been a major factor in the frequency of wildfires during this period.

Many scholars have examined charcoal abundance changes in Quaternary sediments to show that orbital cycle forcing climate drives wildfire activity (Verardo and Ruddiman, 1996; Thevenon et al., 2004; Zhou et al., 2007; Daniau et al., 2013, 2023; Kappenberg et al., 2019; Hao et al., 2020; Shi et al., 2020; Zhang et al., 2023b). Zhou et al. (2023), based on a high-resolution charcoal fragment record from the Wushan Basin of the Tibetan Plateau during the Middle Miocene, found that orbital period (short eccentricity, slope, and age difference) forced climate change to control wildfire activity by influencing the amount of vegetative fuels and their combustibility. In this study, Coal 9 has a floor age of 300.6 ± 1.4 Ma, a roof age of 302.5 ± 1.3 Ma, and a depositional age of ~1.9 Ma (Zhang et al., 2023a). We explored the effect of the orbital cycle on wildfires using long eccentricity. As shown in Fig. 5(b-d), the variation of the long eccentricity had a good correlation with our climatic indicators (CaO/MgO, CaO/MgO • Al_2O_3). The maximum eccentricity is

https://doi.org/10.5194/cp-2024-42
Preprint. Discussion started: 20 June 2024

associated with a warmer and more humid period, while ~~the~~ minimum eccentricity is associated with a colder and dryer period. When the orbital cycle eccentricity is at maximum, the sun was at perihelion ~~and the amount of~~ insolation ~~was relatively abundant~~, leading to a sufficient accumulation of fuels, which in turn led to an increase in wildfire activity (Kappenberg et al., 2019; Hollaar et al., 2021; Qiu et al., 2023; Zhang et al., 2023b). This is consistent with the study by Kappenberg et al. (2019) who found that orbital forcing leads to peak wildfire activity during warm and humid periods.

Combined with the above research, the factors controlling wildfires in this study area are shown in Fig. 8. When the eccentricity was at a minimum, the Earth received insufficient insolation, the climate was cold and dry, and seasonal variations were not evident (Hollaar et al., 2021; Huang et al., 2024). The lack of suitable environments for survival at that time resulted ~~the low amount of~~ vegetation. There may have been a low frequency of wildfires occurring at this stage, which produced less charcoal preserved in the peatland (Fig. 8a). When the eccentricity was at a maximum, the Earth received sufficient insolation, the climate was warm and humid, and seasonal variations were evident (Hollaar et al., 2021; Huang et al., 2024). Suitable environments lead to the proliferation of vegetation, which in turn accumulate large amounts of fuel. More rainfall was also followed by more lightning, leading to increased chances of ignition. Thus there were more frequent wildfires during the period, which produced more charcoal preserved in the peatlands (Fig. 8b). In this study, intensive wildfires did not correlate to peaks in Hg concentrations, and the anomalous enrichment of Hg was most likely due to the frequent volcanic activity occurring at that time. When the ~~volcano erupts~~, the ash can ~~carry~~ large Hg transport (Coufalik et al., 2018). When volcanic ash ~~passes through~~ peatlands, the Hg it carried naturally settles and the strong adsorption of Hg by peatlands leads to anomalous enrichment of Hg at that time (Fig. 8a) (Yudovich and Ketris, 2005).

https://doi.org/10.5194/cp-2024-42
Preprint. Discussion started: 20 June 2024

Climate of the Past Discussions

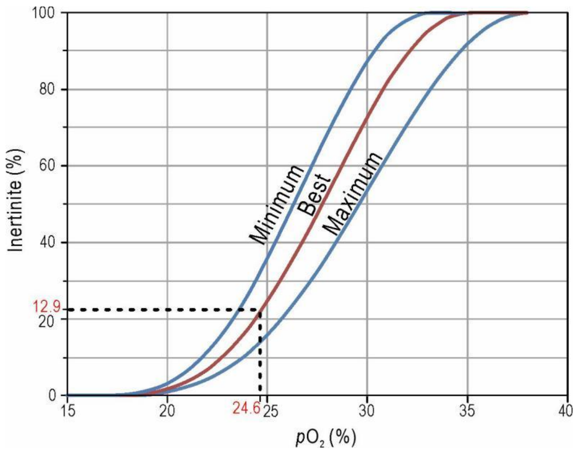

Fig. 7 The atmospheric oxygen concentration during the Late Carboniferous Taiyuan Formation in the Ordos Basin based on the prediction model proposed by Glasspool et al. (2015).

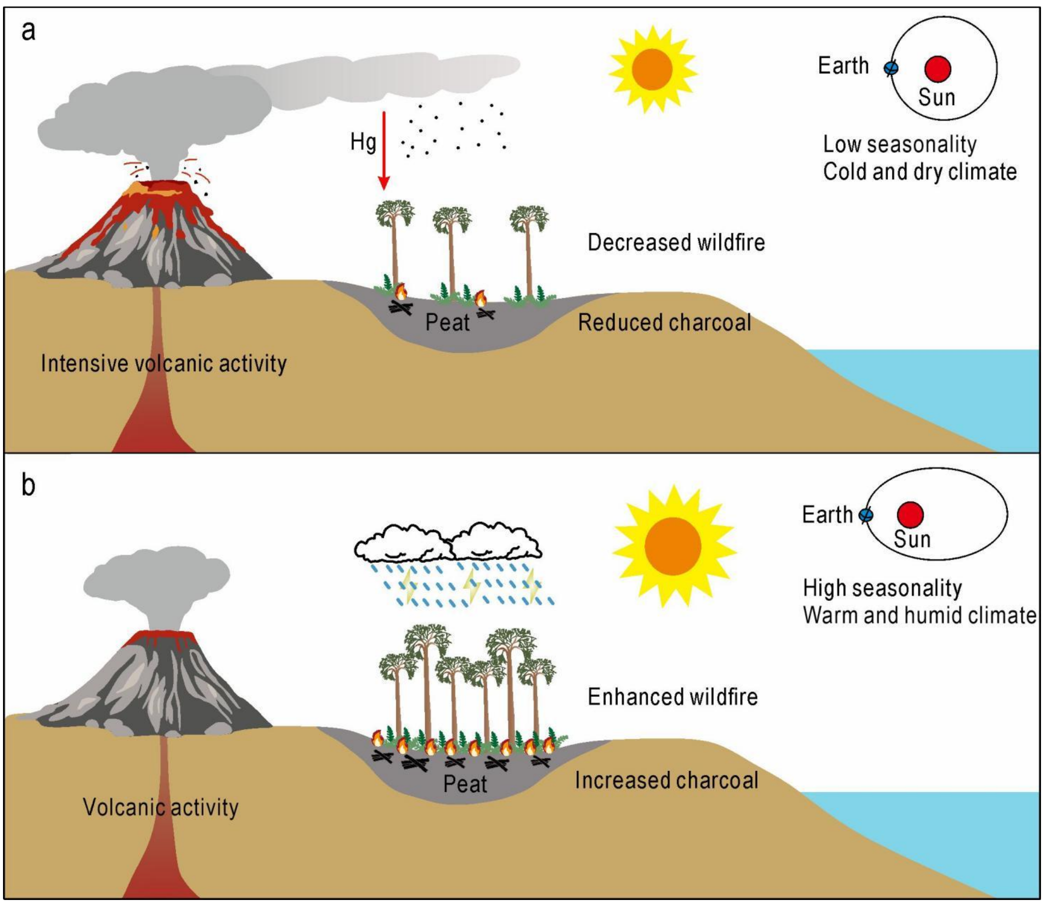

Fig. 8 Illusrtation of wildfires activity forced by the long eccentricity orbital cycle in the study area.

https://doi.org/10.5194/cp-2024-42
Preprint. Discussion started: 20 June 2024

Climate of the Past Discussions

5.3.2 The geographical distribution of published evidence in the Gzhelian

The distribution of wildfires on Earth is not random, and the spatial distribution of wildfires in the modern world is affected by vegetation, climate, topography, and human activities (Krawchuk et al., 2009). Studies have shown that frequent wildfires in modern environments mainly occur in tropical forests and savannas (Mouillot and Field, 2005; Giglio et al., 2006; Flannigan et al., 2009, 2013). In this study, based on the distribution of climate zones published by Boucot et al. (2013), it was found that all of the wildfire records for the Gzhelian occurred in the tropical climate zone (Fig. 9). ~~It was~~ similar to the modern distribution of wildfires. In the tropics of the Gzhelian, different biomes are distributed, mainly divided into humid to semi-humid wetland groups and semi-humid to semi-arid wetland groups, and the peatlands were under alternating humid and dry changing environments (DiMichele et al., 2010; DiMichele, 2014). In warm and humid environments, vegetation ~~grows densely~~ and generates large fuel accumulations. ~~And in~~ arid environments, fuel burnability is enhanced, which in turn promotes more frequent wildfires (Denis et al., 2017; Baker, 2022). Hence the ~~frequent occurrence of~~ wildfires in the tropics ~~with~~ alternating seasons.

~~In view of the spatial distribution~~, the Gzhelian wildfire records were all located at low latitudes near the equator. In the Gzhelian, the southern part of the Gondwana was covered by a large ice sheet, resulting in the lack of vegetation and the lack of fuel needed for wildfires to burn (Scotese, 2021) (Fig. 9). Similarly in the northern part of the Gondwana and the northern part of the Laurasia there were extensive arid climate zones spread across the mainland that lacked the fuels needed for wildfire burning, resulting in the absence of wildfire records (Fig. 9). However, it is worth noting that widespread biases, such as taphonomy, research preferences, and sampling bias, may result in global wildfire data for the Gzhelian ~~not representing the true situation at that time~~ (Brown et al., 2012; Hamad et al., 2012; Lu et al., 2021; Lü et al., 2024). For example, this study

https://doi.org/10.5194/cp-2024-42
Preprint. Discussion started: 20 June 2024

found no evidence of wildfires that have been reported in warm temperate regions (Fig. 9).

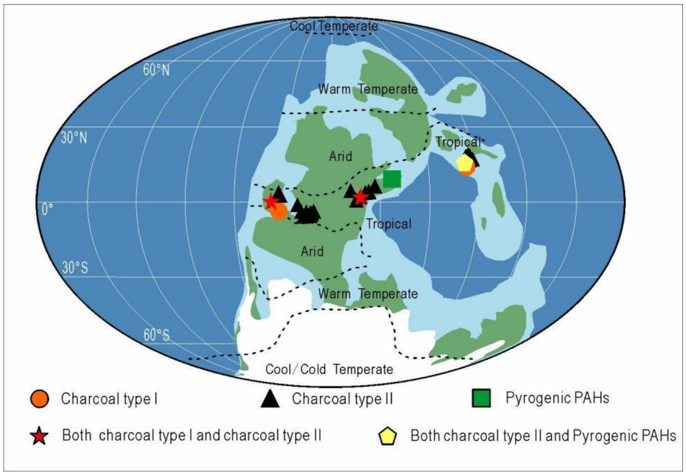

Fig. 9 Paleogeographic distribution of published wildfire occurrences during the Gzhelian. Plate reconstructions from Scotese (2016) with paleoclimatic zones based on Boucot et al. (2013).

6. Conclusion

In this study, the detailed analysis of the inertinite in the No. 9 coal of the Yaogou coal mine in the Ordos Basin, China, demonstrated that frequent wildfires ~~had~~ occurred in the region during the Gzhelian ~~of the Late Carboniferous~~ and were mainly low-temperature fires. The frequency of wildfires during this period may be related to the forcing of the long eccentricity orbital cycle, where changes in the climate due to changes in the orbital cycle affect the fuel load. The review of the global wildfire record of the Gzhelian that wildfires were concentrated in low-latitude tropical climates, and the distribution of wildfires may have been limited by the climate and fuels available at that time. The anomalous enrichment of Hg in No. 9 coal was probably due to inputs of Hg from the frequent volcanic activity occurring at that time, and was not related to wildfire burning. The different types of wildfire burning may limit the release and enrichment of Hg.

Author Contribution

All the authors have actively participated in the preparation of the manuscript. Wenxu Du was responsible for data curation, methodology, and writing; Dawei Lv was responsible for funding acquisition, project administration, and supervision; Zhihui Zhang was responsible for funding acquisition and methodology; Munira Raji was responsible for review; Cuiyu Song was responsible for conceptualization and methodology; Luojing Wang was responsible for visualization and investigation; Zekuan Li was responsible for investigation; Kai Cao was responsible for software and validation; Ruoxiang Yuan was responsible for visualization and investigation; Yuzhuang Sun was responsible for review. All authors read and approved the final proof.

Competing Interests

The authors declare that they have no conflict of interest.

Acknowledgement

This work was financially supported by the National Natural Science Foundation of China (Grant No. 42102127) and the Natural Science Foundation of Shandong Province (Grant No. ZR2021QD087), Shandong University of Science and Technology (Grant No. 2018TDJH101). We think the Deep-Time Digital Earth program (DDE) to support this work. We thank Jincheng Xu to helped with this study. We gratefully acknowledge Professor James C. Hower for his valuable comments on this paper.

References

Ao, W., Huang, W., Weng, C., Xiao, X., Liu, D., Tang, X., Chen, P., Zhao, Z., Wan, H., and Finkelman, R. B.: Coal petrology and genesis of Jurassic coal in the Ordos Basin, China, Geoscience Frontiers, 3, 85-95, https://doi.org/10.1016/j.gsf.2011.09.004, 2012.

Baker, S. J.: Fossil evidence that increased wildfire activity occurs in tandem with periods of global warming in Earth's past, Earth-Science Reviews, 224, 103871, https://doi.org/10.1016/j.earscirev.2021.103871, 2022.

Beeston, J.: Organic petrology of liptinites in the denison trough, Queensland, The APPEA Journal, 27, 86-97, https://doi.org/10.1071/AJ86009, 1987.

Belcher, C. M., and Hudspith, V. A.: Changes to Cretaceous surface fire behaviour influenced the spread of the early angiosperms, New Phytologist, 213, 1521-1532, https://doi.org/10.1111/nph.14264, 2017.

Berner, R. A.: The long-term carbon cycle, fossil fuels and atmospheric composition, Nature, 426, 323-326, https://doi.org/10.1038/nature02131, 2003.

Boucot, A. J., Xu, C., Scotese, C. R., and Morley, R. J.: Phanerozoic paleoclimate: an atlas of lithologic indicators of climate, SEPM (Society for Sedimentary Geology) Tulsa, OK, https://doi.org/10.2110/sepmcsp.11, 2013.

Brovkin, V.: Climate-vegetation interaction, Journal de Physique IV (Proceedings), 57-72, https://doi.org/10.1051/jp4:20020452, 2002.

Brown, S. A., Scott, A. C., Glasspool, I. J., and Collinson, M. E.: Cretaceous wildfires and their impact on the Earth system, Cretaceous research, 36, 162-190, https://doi.org/10.1016/j.cretres.2012.02.008, 2012.

Carlquist, S., and Schneider, E. L.: Vessels in ferns: structural, ecological, and evolutionary significance, American Journal of Botany, 88, 1-13, https://doi.org/10.2307/2657121, 2001.

Chen, J. a., and Wan, G.: Sediment particle size distribution and its environmental significance in Lake Erhai, Yunnan Province, Chinese Journal of Geochemistry, 18, 314-320, https://doi.org/10.1007/bf03052905, 1999.

Cheng, T., Zou, J., Shi, X., Gorbarenko, S., Vasilenko, Y., Bosin, A., Liu, Y., Chen, B., and Cheng, F.: Climate-driven changes in high-intensity wildfire on orbital timescales in Eurasia since 320 Ka, Lithosphere, https://doi.org/10.2113/2022/7562666, 2022.

https://doi.org/10.5194/cp-2024-42
Preprint. Discussion started: 20 June 2024

Coufalík, P., Krmíček, L., Zvěřina, O., Meszarosová, N., Hladil, J., and Komárek, J.: Model of mercury flux associated with volcanic activity, Bulletin of environmental contamination and toxicology, 101, 549-553, https://doi.org/10.1007/s00128-018-2430-5, 2018.

Dai, S., Ren, D., Chou, C.-L., Li, S., and Jiang, Y.: Mineralogy and geochemistry of the no. 6 coal (Pennsylvanian) in the Junger Coalfield, Ordos Basin, China, International Journal of Coal Geology, 66, 253-270, https://doi.org/10.1016/j.coal.2005.08.003, 2006.

Dai, S., Li, D., Chou, C.-L., Zhao, L., Zhang, Y., Ren, D., Ma, Y., and Sun, Y.: Mineralogy and geochemistry of boehmite-rich coals: new insights from the Haerwusu Surface Mine, Jungar Coalfield, Inner Mongolia, China, International journal of coal geology, 74, 185-202, https://doi.org/10.1016/j.coal.2008.01.001, 2008.

Dai, S., Jiang, Y., Ward, C. R., Gu, L., Seredin, V. V., Liu, H., Zhou, D., Wang, X., Sun, Y., and Zou, J.: Mineralogical and geochemical compositions of the coal in the Guanbanwusu Mine, Inner Mongolia, China: Further evidence for the existence of an Al (Ga and REE) ore deposit in the Jungar Coalfield, International Journal of Coal Geology, 98, 10-40, https://doi.org/10.1016/j.coal.2012.03.003, 2012a.

Dai, S., Ren, D., Chou, C.-L., Finkelman, R. B., Seredin, V. V., and Zhou, Y.: Geochemistry of trace elements in Chinese coals: A review of abundances, genetic types, impacts on human health, and industrial utilization, International Journal of Coal Geology, 94, 3-21, https://doi.org/10.1016/j.coal.2011.02.003, 2012b.

Daniau, A.-L., Sánchez Goñi, M. F., Martinez, P., Urrego, D. H., Bout-Roumazeilles, V., Desprat, S., and Marlon, J. R.: Orbital-scale climate forcing of grassland burning in southern Africa, Proceedings of the National Academy of Sciences, 110, 5069-5073, https://doi.org/10.1073/pnas.1214292110, 2013.

https://doi.org/10.5194/cp-2024-42
Preprint. Discussion started: 20 June 2024

Daniau, A.-L., Loutre, M.-F., Swingedouw, D., Laepple, T., Bassinot, F., Malaizé, B., Kageyama, M., Charlier, K., and Carfantan, H.: Precession and obliquity forcing of the South African monsoon revealed by sub-tropical fires, Quaternary Science Reviews, 310, 108128, https://doi.org/10.1016/j.quascirev.2023.108128, 2023.

Daniau, A. L., Bartlein, P. J., Harrison, S., Prentice, I. C., Brewer, S., Friedlingstein, P., Harrison-Prentice, T., Inoue, J., Izumi, K., and Marlon, J.: Predictability of biomass burning in response to climate changes, Global Biogeochemical Cycles, 26, https://doi.org/10.1029/2011GB004249, 2012.

Denis, E. H., Pedentchouk, N., Schouten, S., Pagani, M., and Freeman, K. H.: Fire and ecosystem change in the Arctic across the Paleocene-Eocene Thermal Maximum, Earth and Planetary Science Letters, 467, 149-156, https://doi.org/10.1016/j.epsl.2017.03.021, 2017.

Diessel, C. F.: The stratigraphic distribution of inertinite, International Journal of Coal Geology, 81, 251-268, https://doi.org/10.1016/j.coal.2009.04.004, 2010.

DiMichele, W. A., and Phillips, T. L.: The ecology of Paleozoic ferns, Review of Palaeobotany and Palynology, 119, 143-159, https://doi.org/10.1016/s0034-6667(1)00134-8, 2002.

DiMichele, W. A.: Wetland-dryland vegetational dynamics in the Pennsylvanian ice age tropics, International Journal of Plant Sciences, 175, 123-164, https://doi.org/10.1086/675235, 2014.

Eskanazy, G., Finkelman, R. B., and Chattarjee, S.: Some considerations concerning the use of correlation coefficients and cluster analysis in interpreting coal geochemistry data, International Journal of Coal Geology, 83, 491-493, https://doi.org/10.1016/j.coal.2010.05.006, 2010.

Flannigan, M., Cantin, A. S., De Groot, W. J., Wotton, M., Newbery, A., and Gowman, L. M.: Global wildland fire season severity in the 21st century, Forest Ecology and Management, 294,

https://doi.org/10.5194/cp-2024-42
Preprint. Discussion started: 20 June 2024

Climate of the Past Discussions

54-61, https://doi.org/10.1016/j.foreco.2012.10.022, 2013.

Flannigan, M. D., Krawchuk, M. A., de Groot, W. J., Wotton, B. M., and Gowman, L. M.: Implications of changing climate for global wildland fire, International journal of wildland fire, 18, 483-507, https://doi.org/10.1071/wf08187, 2009.

Giglio, L., Van der Werf, G., Randerson, J., Collatz, G., and Kasibhatla, P.: Global estimation of burned area using MODIS active fire observations, Atmospheric Chemistry and Physics, 6, 957-974, https://doi.org/10.5194/acp-6-957-2006, 2006.

Glasspool, I. J., and Scott, A. C.: Phanerozoic concentrations of atmospheric oxygen reconstructed from sedimentary charcoal, Nature Geoscience, 3, 627-630, https://doi.org/10.1038/ngeo923, 2010.

Glasspool, I. J., Scott, A. C., Waltham, D., Pronina, N., and Shao, L.: The impact of fire on the Late Paleozoic Earth system, Frontiers in Plant Science, 6, 756, https://doi.org/10.3389/fpls.2015.00756, 2015.

Grigal, D.: Mercury sequestration in forests and peatlands: a review, Journal of environmental quality, 32, 393-405, https://doi.org/10.2134/jeq2003.0393, 2003.

Guo, Y., and Bustin, R.: FTIR spectroscopy and reflectance of modern charcoals and fungal decayed woods: implications for studies of inertinite in coals, International Journal of Coal Geology, 37, 29-53, https://doi.org/10.1016/s0166-5162（98）00019-6, 1998.

Hamad, A. M. A., Jasper, A., and Uhl, D.: The record of Triassic charcoal and other evidence for palaeo-wildfires: signal for atmospheric oxygen levels, taphonomic biases or lack of fuel?, International Journal of Coal Geology, 96, 60-71, https://doi.org/10.1016/j.coal.2012.03.006, 2012.

Hao, Y., Han, Y., An, Z., and Burr, G. S.: Climatic control of orbital time-scale wildfire occurrences since the late MIS 3 at Qinghai Lake, monsoon marginal zone, Quaternary international, 550, 20-26, https://doi.org/10.1016/j.quaint.2020.03.002, 2020.

Hollaar, T. P., Baker, S. J., Hesselbo, S. P., Deconinck, J.-F., Mander, L., Ruhl, M., and Belcher, C. M.: Wildfire activity enhanced during phases of maximum orbital eccentricity and precessional forcing in the Early Jurassic, Communications Earth & Environment, 2, 247, https://doi.org/10.1038/s43247-021-00307-3, 2021.

Hou, H., Shao, L., Liang, G., Tang, Y., Zhang, H., and Zhang, J.: Repeated wildfires in the middle jurassic Xishanyao formation (aalenian and bajocian ages) in northwestern China, Acta Geologica Sinica-English Edition, 96, 1752-1763, https://doi.org/10.1111/1755-6724.14912, 2022.

Hower, J. C., Eble, C. F., Hopps, S. D., and Morgan, T. D.: Aspects of rare earth element geochemistry of the Pond Creek coalbed, Pike County, Kentucky, International Journal of Coal Geology, 261, 104082, https://doi.org/10.1016/j.coal.2022.104082, 2022.

Huang, H., Fang, Q., Huang, W., Shi, M., Zhang, S., Yang, T., Li, H., and Wu, H.: A short-term warming interval during the apex of the late Paleozoic Ice Age: Evidence from geochemical and magnetic records from South China, Palaeogeography, Palaeoclimatology, Palaeoecology, 112178, https://doi.org/10.1016/j.palaeo.2024.112178, 2024.

Hudspith, V., Scott, A., Collinson, M., Pronina, N., and Beeley, T.: Evaluating the extent to which wildfire history can be interpreted from inertinite distribution in coal pillars: An example from the Late Permian, Kuznetsk Basin, Russia, International Journal of Coal Geology, 89, 13-25, https://doi.org/10.1016/j.coal.2011.07.009, 2012.

Hudspith, V. A., and Belcher, C. M.: Some semifusinite in coal may form during diagenesis, not wildfires, International Journal of Coal Geology, 218, 103360,

https://doi.org/10.5194/cp-2024-42
Preprint. Discussion started: 20 June 2024

https://doi.org/10.1016/j.coal.2019.103360, 2020.

Jasper, A., Guerra-Sommer, M., Hamad, A. M. A., Bamford, M., Bernardes-de-Oliveira, M. E. C., Tewari, R., and Uhl, D.: The burning of Gondwana: Permian fires on the southern continent—A palaeobotanical approach, Gondwana Research, 24, 148-160, https://doi.org/10.1016/j.gr.2012.08.017, 2013.

Jasper, A., Pozzebon-Silva, Â., Carniere, J. S., and Uhl, D.: Palaeozoic and Mesozoic palaeo-wildfires: An overview on advances in the 21st Century, Journal of Palaeosciences, 70, 159-172, https://doi.org/10.54991/jop.2021.13, 2021.

Jinhua, F., Shixiang, L., Liming, X., and Xiaobing, N.: Paleo-sedimentary environmental restoration and its significance of Chang 7 Member of Triassic Yanchang Formation in Ordos Basin, NW China, Petroleum Exploration and Development, 45, 998-1008, https://doi.org/10.1016/s1876-3804（18）30104-6, 2018.

Jones, T. P., and Chaloner, W. G.: Fossil charcoal, its recognition and palaeoatmospheric significance, Palaeogeography, Palaeoclimatology, Palaeoecology, 97, 39-50, https://doi.org/10.1016/0031-0182（91）90180-y, 1991.

Jones, T. P.: Fusain in late jurassic sediments from the witch ground graben, North sea, UK, in: 4th European Palaeobotanical and Palynological Conference, Heerlen/Kerkrade, The Netherlands, 19-23 September 1994, 99-104, 1997.

Kappenberg, A., Lehndorff, E., Pickarski, N., Litt, T., and Amelung, W.: Solar controls of fire events during the past 600,000 years, Quaternary Science Reviews, 208, 97-104, https://doi.org/10.1016/j.quascirev.2019.02.008, 2019.

Kortenski, J., and Sotirov, A.: Trace and major element content and distribution in Neogene lignite from the Sofia Basin, Bulgaria, International Journal of Coal Geology, 52, 63-82,

https://doi.org/10.5194/cp-2024-42
Preprint. Discussion started: 20 June 2024

https://doi.org/10.1016/s0166-5162(02)00133-7, 2002.

Krawchuk, M. A., Moritz, M. A., Parisien, M.-A., Van Dorn, J., and Hayhoe, K.: Global pyrogeography: the current and future distribution of wildfire, PloS one, 4, e5102, https://doi.org/10.1371/journal.pone.0005102, 2009.

Ku, P., Tsui, M. T.-K., Nie, X., Chen, H., Hoang, T. C., Blum, J. D., Dahlgren, R. A., and Chow, A. T.: Origin, reactivity, and bioavailability of mercury in wildfire ash, Environmental science & technology, 52, 14149-14157, https://doi.org/10.1021/acs.est.8b03729, 2018.

Li, Y., Tang, D., Wu, P., Niu, X., Wang, K., Qiao, P., and Wang, Z.: Continuous unconventional natural gas accumulations of Carboniferous-Permian coal-bearing strata in the Linxing area, northeastern Ordos basin, China, Journal of Natural Gas Science and Engineering, 36, 314-327, https://doi.org/10.1016/j.jngse.2016.10.037, 2016.

Litt, T., Pickarski, N., Heumann, G., Stockhecke, M., and Tzedakis, P. C.: A 600,000 year long continental pollen record from Lake Van, eastern Anatolia (Turkey), Quaternary Science Reviews, 104, 30-41, https://doi.org/10.1016/j.quascirev.2014.03.017, 2014.

Liu, B., Jin, H., Sun, L., Sun, Z., and Su, Z.: Winter and summer monsoonal evolution in northeastern Qinghai-Tibetan Plateau during the Holocene period, Geochemistry, 73, 309-321, https://doi.org/10.1016/j.chemer.2013.03.006, 2013.

Liu, B., Spiekermann, R., Zhao, C., Puettmann, W., Sun, Y., Jasper, A., and Uhl, D.: Evidence for the repeated occurrence of wildfires in an upper Pliocene lignite deposit from Yunnan, SW China, International Journal of Coal Geology, 250, 103924, https://doi.org/10.1016/j.coal.2021.103924, 2022.

Lü, D.-W., Du, W.-X., Zhang, Z.-H., Gao, Y., Wang, T.-T., Xu, J.-C., Zhang, A.-C., and Wang, C.-S.: A synthesis of the Cretaceous wildfire record related to atmospheric oxygen levels?, Journal of

https://doi.org/10.5194/cp-2024-42
Preprint. Discussion started: 20 June 2024

Palaeogeography, 13, 149-164, https://doi.org/10.1016/j.jop.2023.10.001, 2024.

Lu, M., Ikejiri, T., and Lu, Y.: A synthesis of the Devonian wildfire record: Implications for paleogeography, fossil flora, and paleoclimate, Palaeogeography, Palaeoclimatology, Palaeoecology, 571, 110321, https://doi.org/10.1016/j.palaeo.2021.110321, 2021.

Marlon, J. R., Bartlein, P. J., Daniau, A.-L., Harrison, S. P., Maezumi, S. Y., Power, M. J., Tinner, W., and Vanniére, B.: Global biomass burning: a synthesis and review of Holocene paleofire records and their controls, Quaternary Science Reviews, 65, 5-25, https://doi.org/10.1016/j.quascirev.2012.11.029, 2013.

McParland, L. C., Collinson, M. E., Scott, A. C., and Campbell, G.: The use of reflectance values for the interpretation of natural and anthropogenic charcoal assemblages, Archaeological and Anthropological Sciences, 1, 249-261, https://doi.org/10.1007/s12520-009-0018-z, 2009.

Mouillot, F., and Field, C. B.: Fire history and the global carbon budget: a 1 × 1 fire history reconstruction for the 20th century, Global Change Biology, 11, 398-420, https://doi.org/10.1111/j.1365-2486.2005.00920.x, 2005.

Osterkamp, I. C., Lara, D. M. d., Gonçalves, T. A. P., Kauffmann, M., Périco, E., Stülp, S., Machado, N. T. G., Uhl, D., and Jasper, A.: Changes of wood anatomical characters of selected species of Araucaria-during artificial charring-implications for palaeontology, Acta Botanica Brasilica, 32, 198-211, https://doi.org/10.1590/0102-33062017abb0360, 2017.

Pavlish, J. H., Sondreal, E. A., Mann, M. D., Olson, E. S., Galbreath, K. C., Laudal, D. L., and Benson, S. A.: Status review of mercury control options for coal-fired power plants, Fuel processing technology, 82, 89-165, https://doi.org/10.1016/S0378-3820（03）00059-6, 2003.

Petersen, H. I., and Lindström, S.: Synchronous wildfire activity rise and mire deforestation at the Triassic-Jurassic boundary, https://doi.org/10.1371/journal.pone.0047236, 2012.

Presswood, S. M., Rimmer, S. M., Anderson, K. B., and Filiberto, J.: Geochemical and petrographic alteration of rapidly heated coals from the Herrin (No. 6) Coal Seam, Illinois Basin, International Journal of Coal Geology, 165, 243-256, https://doi.org/10.1016/j.coal.2016.08.022, 2016.

Pyle, D. M., and Mather, T. A.: The importance of volcanic emissions for the global atmospheric mercury cycle, Atmospheric Environment, 37, 5115-5124, https://doi.org/10.1016/j.atmosenv.2003.07.011, 2003.

Qiu, R., Fang, L., Lv, P., Jiang, F., Zhang, X., Zhang, X., Zhang, P., Zhu, L., and Shi, S.: Long eccentricity forcing of the Late Pliensbachian to Early Toarcian (Jurassic) terrestrial wildfire activities in the Tarim Basin, northwestern China, Palaeogeography, Palaeoclimatology, Palaeoecology, 613, 111408, https://doi.org/10.1016/j.palaeo.2023.111408, 2023.

Robson, B. E., Collinson, M. E., Riegel, W., Wilde, V., Scott, A. C., and Pancost, R. D.: Early Paleogene wildfires in peat-forming environments at Schöningen, Germany, Palaeogeography, Palaeoclimatology, Palaeoecology, 437, 53-62, https://doi.org/10.1016/j.palaeo.2015.07.016, 2015.

Roos-Barraclough, F., Martinez-Cortizas, A., García-Rodeja, E., and Shotyk, W.: A 14 500 year record of the accumulation of atmospheric mercury in peat: volcanic signals, anthropogenic influences and a correlation to bromine accumulation, Earth and Planetary Science Letters, 202, 435-451, https://doi.org/10.1016/s0012-821x（02）00805-1, 2002.

Schneider, E. L., and Carlquist, S.: SEM studies on vessels in ferns. 17. Psilotaceae, American Journal of Botany, 87, 176-181, https://doi.org/10.2307/2656903, 2000.

Scotese, C.: The PALEOMAP Project PaleoAtlas for ArcGIS, version 1, Volume, 2, 16-31, 2008.

Scotese, C. R.: An atlas of Phanerozoic paleogeographic maps: the seas come in and the seas go out, Annual Review of Earth and Planetary Sciences, 49, 679-728, https://doi.org/10.1146/annurev-earth-081320-064052, 2021.

Scott, A. C., and Jones, T. P.: Fossil charcoal: a plant-fossil record preserved by fire, Geology Today, 7, 214-216, https://doi.org/10.1111/j.1365-2451.1991.tb00806.x, 1991.

Scott, A. C.: The Pre-Quaternary history of fire, Palaeogeography, palaeoclimatology, palaeoecology, 164, 281-329, https://doi.org/10.1016/s0031-0182（00）00192-9, 2000.

Scott, A. C., and Glasspool, I. J.: The diversification of Paleozoic fire systems and fluctuations in atmospheric oxygen concentration, Proceedings of the National Academy of Sciences, 103, 10861-10865, https://doi.org/10.1073/pnas.0604090103, 2006.

Scott, A. C., and Glasspool, I. J.: Observations and experiments on the origin and formation of inertinite group macerals, International Journal of Coal Geology, 70, 53-66, https://doi.org/10.1016/j.coal.2006.02.009, 2007.

Scott, A. C.: Charcoal recognition, taphonomy and uses in palaeoenvironmental analysis, Palaeogeography, Palaeoclimatology, Palaeoecology, 291, 11-39, https://doi.org/10.1016/j.palaeo.2009.12.012, 2010.

Scott, A. C.: Fire: A Very Short Introduction, Oxford University Press, Great Clarendon Street, Oxford, OX2 6DP,United Kingdom, https://doi.org/10.1093/actrade/9780198830030.001.0001, 2020.

Scott, A. C.: Charcoalified vegetation from the Pennsylvanian of Yorkshire, England: Implications for the interpretation of Carboniferous wildfires, Review of Palaeobotany and Palynology, 296, https://doi.org/10.1016/j.revpalbo.2021.104540, 104540, 2022.

Selin, N. E.: Global biogeochemical cycling of mercury: a review, Annual review of environment and resources, 34, 43-63, https://doi.org/10.1146/annurev.environ.051308.084314, 2009.

https://doi.org/10.5194/cp-2024-42
Preprint. Discussion started: 20 June 2024

Shen, J., Feng, Q., Algeo, T. J., Liu, J., Zhou, C., Wei, W., Liu, J., Them II, T. R., Gill, B. C., and Chen, J.: Sedimentary host phases of mercury (Hg) and implications for use of Hg as a volcanic proxy, Earth and Planetary Science Letters, 543, 116333, https://doi.org/10.1016/j.epsl.2020.116333, 2020.

Shen, W., Zhao, Q., Uhl, D., Wang, J., and Sun, Y.: Wildfire activity and impacts on palaeoenvironments during the late Paleozoic Ice Age-New data from the North China Basin, Palaeogeography, Palaeoclimatology, Palaeoecology, 629, 111781, https://doi.org/10.1016/j.palaeo.2023.111781, 2023.

Shi, Y., Pan, B., Wei, M., Li, X., Cai, M., Wang, J., Xu, X., Hu, J., and Shi, W.: Wildfire evolution and response to climate change in the Yinchuan Basin during the past 1.5 Ma based on the charcoal records of the PL02 core, Quaternary Science Reviews, 241, 106393, https://doi.org/10.1016/j.quascirev.2020.106393, 2020.

Stockhecke, M., Timmermann, A., Kipfer, R., Haug, G. H., Kwiecien, O., Friedrich, T., Menviel, L., Litt, T., Pickarski, N., and Anselmetti, F. S.: Millennial to orbital-scale variations of drought intensity in the Eastern Mediterranean, Quaternary Science Reviews, 133, 77-95, https://doi.org/10.1016/j.quascirev.2015.12.016, 2016.

Sun, Q., Wang, S., Zhou, J., Chen, Z., Shen, J., Xie, X., Wu, F., and Chen, P.: Sediment geochemistry of Lake Daihai, north-central China: implications for catchment weathering and climate change during the Holocene, Journal of Paleolimnology, 43, 75-87, https://doi.org/10.1007/s10933-009-9315-x, 2010.

Sun, R., Sonke, J. E., and Liu, G.: Biogeochemical controls on mercury stable isotope compositions of world coal deposits: A review, Earth-science reviews, 152, 1-13, https://doi.org/10.1016/j.earscirev.2015.11.005, 2016.

https://doi.org/10.5194/cp-2024-42
Preprint. Discussion started: 20 June 2024

Swain, D. L.: A shorter, sharper rainy season amplifies California wildfire risk, Geophysical Research Letters, 48, e2021GL092843, https://doi.org/10.1029/2021gl092843, 2021.

Teichmüller, M.: The genesis of coal from the viewpoint of coal petrology, International Journal of Coal Geology, 12, 1-87, https://doi.org/10.1016/0166-5162（89）90047-5, 1989.

Thevenon, F., Bard, E., Williamson, D., and Beaufort, L.: A biomass burning record from the West Equatorial Pacific over the last 360 ky: methodological, climatic and anthropic implications, Palaeogeography, Palaeoclimatology, Palaeoecology, 213, 83-99, https://doi.org/10.1016/s0031-0182（04）00364-5, 2004.

Turetsky, M. R., Harden, J. W., Friedli, H. R., Flannigan, M., Payne, N., Crock, J., and Radke, L.: Wildfires threaten mercury stocks in northern soils, Geophysical research letters, 33, https://doi.org/10.1029/2005gl025595, 2006.

Uhl, D., Spiekermann, R., Wuttke, M., Poschmann, M. J., and Jasper, A.: Wildfires during the Paleogene (late Eocene – late Oligocene) of the Neuwied Basin (W-Germany), Review of Palaeobotany and Palynology, 297, 104565, https://doi.org/10.1016/j.revpalbo.2021.104565, 2022.

Varma, A.: Influence of petrographical composition on coking behavior of inertinite-rich coals, International journal of coal geology, 30, 337-347, https://doi.org/10.1016/0166-5162（95）00053-4, 1996.

Verardo, D. J., and Ruddiman, W. F.: Late Pleistocene charcoal in tropical Atlantic deep-sea sediments: climatic and geochemical significance, Geology, 24, 855-857, https://doi.org/10.1130/0091-7613（1996）024<0855：LPCITA>2.3.co;2, 1996.

Wang, C. a., Liu, Y., Zhang, X., and Che, D.: A study on coal properties and combustion characteristics of blended coals in northwestern China, Energy & Fuels, 25, 3634-3645,

https://doi.org/10.5194/cp-2024-42
Preprint. Discussion started: 20 June 2024

https://doi.org/10.1021/ef200686d, 2011.

Wang, S.: Ordos basin superposed evolution and structural controls of coal forming activities, Earth Science Frontiers, 24, 54-63, https://10.13745/j.esf.yx.2016-12-11, 2017. (in Chinese).

Wang, X., Yuan, W., Lin, C.-J., Zhang, L., Zhang, H., and Feng, X.: Climate and vegetation as primary drivers for global mercury storage in surface soil, Environmental Science & Technology, 53, 10665-10675, https://doi.org/10.1021/acs.est.9b02386, 2019.

Woerndle, G. E., Tsz-Ki Tsui, M., Sebestyen, S. D., Blum, J. D., Nie, X., and Kolka, R. K.: New insights on ecosystem mercury cycling revealed by stable isotopes of mercury in water flowing from a headwater peatland catchment, Environmental science & technology, 52, 1854-1861, https://doi.org/10.1021/acs.est.7b04449, 2018.

Xie, W., Tan, J., Wang, W., Jia, J., Liu, Z., Wu, J., Wang, Y., and Song, X.: Record of Middle Jurassic wildfire and its incidental mercury emissions in northern Qaidam Basin, China: Evidence from the inertinite and mercury anomalies in coal, International Journal of Coal Geology, 261, 104078, https://doi.org/10.2139/ssrn.4105730, 2022.

Xu, Y., Uhl, D., Zhang, N., Zhao, C., Qin, S., Liang, H., and Sun, Y.: Evidence of widespread wildfires in coal seams from the Middle Jurassic of Northwest China and its impact on paleoclimate, Palaeogeography, Palaeoclimatology, Palaeoecology, 559, 109819, https://doi.org/10.1016/j.palaeo.2020.109819, 2020.

Yudovich, Y. E., and Ketris, M.: Mercury in coal: A review: Part 1. Geochemistry, International Journal of Coal Geology, 62, 107-134, https://doi.org/10.1016/s0140-6701（06）81438-4, 2005.

Yunker, M. B., Macdonald, R. W., Vingarzan, R., Mitchell, R. H., Goyette, D., and Sylvestre, S.: PAHs in the Fraser River basin: a critical appraisal of PAH ratios as indicators of PAH source and composition, Organic geochemistry, 33, 489-515, https://doi.org/10.1016/s0146-6380（02）

00002-5, 2002.

Zhang, X., Li, S., Zhao, X., Geng, G., and Yan, M.: The sedimentary environment of Early Cretaceous rift basin in eastern China and its response to the Faraoni event, Geosciences Journal, 24, 359-377, https://doi.org/10.1007/s12303-019-0031-x, 2020a.

Zhang, X., Gao, Z., Fan, T., Xue, J., Li, W., Cao, F., and Zhang, H.: Geochemical characteristics, provenance and paleodepostional environment of the Lower Jurassic Huxishan Formation in the Lenghu area, northwestern Qaidam Basin, North West China: Implications for organic matter origin, Journal of Petroleum Science and Engineering, 205, 108951, https://doi.org/10.1016/j.petrol.2021.108951, 2021.

Zhang, Z.-H., Lü, D.-W., Wang, T.-T., An, D.-Z., Liu, H.-Y., Wang, D.-D., and Wang, C.-S.: Intensive peatland wildfires during the Aptian-Albian oceanic anoxic event 1b: Evidence from borehole SK-2 in the Songliao Basin, NE China, Journal of Palaeogeography, 11, 448-467, https://doi.org/10.1016/j.jop.2022.06.002, 2022.

Zhang, Z., Wang, C., Lv, D., Hay, W. W., Wang, T., and Cao, S.: Precession-scale climate forcing of peatland wildfires during the early middle Jurassic greenhouse period, Global and planetary change, 184, 103051, https://doi.org/10.1016/j.gloplacha.2019.103051, 2020b.

Zhang, Z., Lv, D., Hower, J. C., Wang, L., Shen, Y., Zhang, A., Xu, J., and Gao, J.: Geochronology, mineralogy, and geochemistry of tonsteins from the Pennsylvanian Taiyuan Formation of the Jungar Coalfield, Ordos Basin, North China, International Journal of Coal Geology, 267, 104183, https://doi.org/10.1016/j.coal.2023.104183, 2023a.

Zhang, Z., Lv, D., Lu, M., Yu, Z., Gao, Y., Wang, T., Gao, J., and Wang, C.: Wildfire activity driven by the 405-kyr orbital climate cycles in the Middle Jurassic, Global and Planetary Change, 222, 104069, https://doi.org/10.1016/j.gloplacha.2023.104069, 2023b.

https://doi.org/10.5194/cp-2024-42
Preprint. Discussion started: 20 June 2024

Zhao, C., Zhang, K., Xiao, L., Uhl, D., Shi, Z., Zhao, W., Zhao, Q., Sun, Y., and Liu, B.: Paleoclimate-induced wildfires in a paleomire in the Ordos Basin, Northern China during the Middle Jurassic greenhouse period, Chemical Geology, 637, 121677, https://doi.org/10.1016/j.chemgeo.2023.121677, 2023.

Zheng, L., Sun, R., Hintelmann, H., Zhu, J., Wang, R., and Sonke, J. E.: Mercury stable isotope compositions in magmatic-affected coal deposits: New insights to mercury sources, migration and enrichment, Chemical Geology, 479, 86-101, https://doi.org/10.1016/j.chemgeo.2017.12.032, 2018.

Zhou, B., Shen, C., Sun, W., Zheng, H., Yang, Y., Sun, Y., and An, Z.: Elemental carbon record of paleofire history on the Chinese Loess Plateau during the last 420 ka and its response to environmental and climate changes, Palaeogeography, Palaeoclimatology, Palaeoecology, 252, 617-625, https://doi.org/10.1016/j.palaeo.2007.05.014, 2007.

Zhou, X., Hui, Z., Vachula, R. S., Wei, X., Chen, P., Zhang, J., Wang, X., and Peng, T.: Mid-Miocene palaeofire and its complex relationship with vegetation changes in the Wushan Basin, northeastern Tibetan Plateau, China: Evidence from a high-resolution charcoal record, Paleoceanography and Paleoclimatology, 38, e2022PA004461, https://doi.org/10.1029/2022pa004461, 2023.